

**Universität
Stuttgart**

**Fachbereich
Mathematik**

A Relaxation Riemann Solver for
Compressible Two-Phase Flow with
Phase Transition and Surface Tension

Christian Rohde, Christoph Zeiler

Preprint 2013/014

**Universität
Stuttgart**

**Fachbereich
Mathematik**

A Relaxation Riemann Solver for
Compressible Two-Phase Flow with
Phase Transition and Surface Tension

Christian Rohde, Christoph Zeiler

Preprint 2013/014

Fachbereich Mathematik
Fakultät Mathematik und Physik
Universität Stuttgart
Pfaffenwaldring 57
D-70 569 Stuttgart

E-Mail: preprints@mathematik.uni-stuttgart.de
WWW: <http://www.mathematik.uni-stuttgart.de/preprints>

ISSN **1613-8309**

© Alle Rechte vorbehalten. Nachdruck nur mit Genehmigung des Autors.
L^AT_EX-Style: Winfried Geis, Thomas Merkle

Abstract

The dynamics of two-phase flows depend crucially on interfacial effects like surface tension and phase transition. A numerical method for compressible inviscid flows is proposed that accounts in particular for these two effects. The approach relies on the solution of Riemann-like problems across the interface that separates the liquid and the vapour phase. Since the analytical solutions of the Riemann problems are only known in particular cases an approximative Riemann solver for arbitrary settings is constructed. The approximative solutions rely on the relaxation technique.

The local well-posedness of the approximative solver is proven. Finally we present numerical experiments for radially symmetric configurations that underline the reliability and efficiency of the numerical scheme.

Keywords: Compressible Two-Phase Flow, Conservation Laws, Riemann Solvers, Bubble and Droplet Dynamics

1 Introduction

We consider the direct numerical simulation of a homogeneous compressible fluid that can appear in a liquid and in a vapour state. In particular we are interested in inviscid two-phase flows that account for surface tension as well as for mass exchange by evaporation and condensation.

The compressible hydrodynamics in the bulk phases is governed for the inviscid case by the Euler equations. The two-phase modelling is much more challenging because possible curvature and phase transition effects induce a complex transfer of momentum and energy through the interface. We follow here a sharp interface approach such that the spatial domain is partitioned into two bulk regions by a free boundary. The flow equations in each bulk region are coupled by appropriate trace conditions. The sharp interface approach is classical in multiphase fluid dynamics, and many numerical methods have been suggested. We consider here a heterogeneous multiscale method (HMM) in the spirit of e.g. [20]. The dynamics in the bulk phases is given by a macroscale model and the local evolution of the interface is determined from a microscale model. The notion of scales in this case should not be mixed up with different spatial or temporal scales. Rather the HMM provides a versatile tool to treat the liquid-vapour free boundary value problem because the complex models for the dynamics of the phase boundary can be realized in the microscale model. Preliminary work in this direction can be found in [9, 12], and for a comparable situation in porous media flow in [13].

Let us give an outline of this paper's content. In Section 2 we present the full mathematical model as a free boundary value problem in arbitrary spatial dimension. We consider the physically most relevant case of slow subsonic phase boundaries such that a Gibbs-Thomson like relation has to be added to the classical coupling conditions (conservation of mass, dynamical Young-Laplace law). Two choices for these conditions that determine the evolution of the interface are proposed.

As a microscale model we obtain a planar Riemann problem, independent of the original spatial dimension. The initial states for the Riemann problem are in different phases. Such Riemann problems have been intensively studied in the last twenty years (see [14] for the general theory and [10] for a recent contribution). However, there are no explicit results for arbitrary pressure relations, kinetic relations and curvature dependent flow. Therefore we will follow [3] and construct in Section 3 an approximative Riemann solver which belongs to the class of relaxation solvers. This approximate Riemann solver is the major new contribution of this paper. With Theorems 3.1 and 3.2 we give basic well-posedness statements for the two kinetic relations under consideration. We believe however that the relaxation approach remains effective for even more general kinetic relations.

In Section 4 we discuss the complete heterogeneous multiscale method for radially symmetric domains. The extension to arbitrary configurations in multiple space dimensions will be presented elsewhere. The overall method is summarised in Algorithm 4.2. Most notably the algorithm guarantees the conservation of mass. Finally in Section 5 we show numerical results. Convergence studies and long term simulations demonstrate the reliability of the overall method. In particular

we show that the numerical method dissipates the associated physical entropy. Furthermore we present a detailed study on curvature effects, and we compare the mass transfer across the interface for different mobilities in the kinetic relations.

2 The mathematical model

2.1 A free boundary value problem for compressible liquid-vapour flow

As the basic modelling approach we consider a sharp interface ansatz. To introduce the precise setting let $\Omega \subset \mathbb{R}^d$ with $d \in \mathbb{N}$ be an open bounded set. For any $t \in [0, T]$, $T > 0$, we assume that Ω is partitioned into the union of two open sets $\Omega_{\text{vap}}(t)$, $\Omega_{\text{liq}}(t)$, which contain the two bulk phases, and a hypersurface $\Gamma(t)$ – the sharp interface –, that separates the two spatial bulk sets. We restrict ourselves to isothermal motion at constant temperature $\theta > 0$, and let the fluid be inviscid. In the spatial-temporal bulk sets $\{(\mathbf{x}, t) \in \Omega \times (0, T) \mid \mathbf{x} \in \Omega_{\text{vap}}(t) \cup \Omega_{\text{liq}}(t)\}$ the dynamics of the fluid is then governed by the hydromechanical system

$$\begin{aligned} \varrho_t + \operatorname{div}(\varrho \mathbf{v}) &= 0, \\ (\varrho \mathbf{v})_t + \operatorname{div}(\varrho \mathbf{v} \otimes \mathbf{v} + \tilde{p}(\varrho) \mathbf{I}) &= \mathbf{0}. \end{aligned} \tag{1}$$

Here $\varrho = \varrho(\mathbf{x}, t) > 0$ denotes the unknown density field and $\mathbf{v} = \mathbf{v}(\mathbf{x}, t) = (v_1(\mathbf{x}, t), \dots, v_d(\mathbf{x}, t))^t \in \mathbb{R}^d$ the unknown velocity field. The pressure $\tilde{p} = \tilde{p}(\varrho)$ is a given scalar function and $\mathbf{I} \in \mathbb{R}^{d \times d}$ the d -dimensional unit matrix.

Before we proceed with the thermodynamical set-up for (1) let us add initial and boundary conditions. We fix the initial position of the interface $\Gamma(0)$ and assume for initial density ϱ_0 und velocity field \mathbf{v}_0

$$\varrho(\mathbf{x}, 0) = \varrho_0(\mathbf{x}), \quad \mathbf{v}(\mathbf{x}, 0) = \mathbf{v}_0(\mathbf{x}) \quad \text{for } \mathbf{x} \in \Omega_{\text{vap}}(0) \cup \Omega_{\text{liq}}(0). \tag{2}$$

For the sake of simplicity we exclude flow across the boundary $\partial\Omega$, i.e.

$$\mathbf{v} \cdot \mathbf{n} = \mathbf{0} \text{ on } \partial\Omega, \tag{3}$$

where \mathbf{n} is the outer normal to $\partial\Omega$.

We denote the specific volume by $\tau = 1/\varrho$ and remark that the pressure $p(\tau) = \tilde{p}(1/\tau)$ is related to the Helmholtz free energy $\psi = \psi(\tau)$ and the chemical potential $\mu = \mu(\tau)$ by

$$p(\tau) = -\psi'(\tau) \text{ and } \mu(\tau) = \psi(\tau) + p(\tau) \tau. \tag{4}$$

As a prototype example we consider here the van der Waals pressure

$$\tilde{p}(\varrho) = \frac{R\theta\varrho}{1-b\varrho} - a\varrho^2 \quad \text{for } \varrho \in (0, b^{-1}),$$

with the specific choices

$$\theta = 0.85, \quad a = 3, \quad b = 1/3 \quad \text{and} \quad R = 8/3. \tag{5}$$

From the graph in Figure 1 we observe that \tilde{p} is increasing in the intervals $\tilde{\mathcal{A}}_{\text{vap}} := (0, \varrho_{\text{vap}}^{\text{spinod}})$ and $\tilde{\mathcal{A}}_{\text{liq}} := (\varrho_{\text{liq}}^{\text{spinod}}, b^{-1})$ which define the vapor and the liquid phase. For later use we introduce also $\mathcal{A}_{\text{vap}} := (1/\varrho_{\text{vap}}^{\text{spinod}}, \infty)$ and $\mathcal{A}_{\text{liq}} := (b, 1/\varrho_{\text{liq}}^{\text{spinod}})$.

The system (1) can be written for $\mathbf{U} = (\varrho, \varrho v_1, \dots, \varrho v_d)^t$ in the conservation form

$$\mathbf{U}_t + \mathbf{F}^1(\mathbf{U})_{x_1} + \dots + \mathbf{F}^d(\mathbf{U})_{x_d} = \mathbf{0},$$

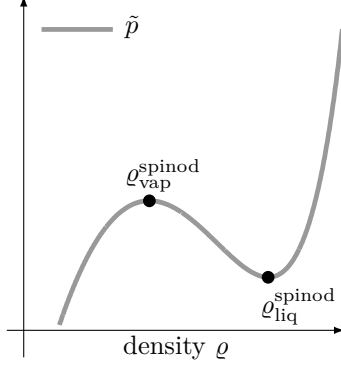


Figure 1: Van der Waals pressure function $\tilde{p} = \tilde{p}(\varrho)$.

with appropriately defined fluxes $\mathbf{F}^1, \dots, \mathbf{F}^d$. For $\boldsymbol{\mu} \in \mathbb{S}^{d-1}$ and $\mathbf{U} \in (0, b^{-1}) \times \mathbb{R}^d$ the eigenvalues of the Jacobian of the directional flux $\mu_1 \mathbf{F}^1(\mathbf{U}) + \dots + \mu_d \mathbf{F}^d(\mathbf{U})$ are then given by

$$\begin{aligned}\lambda_1(\mathbf{U}; \boldsymbol{\mu}) &= \mathbf{v} \cdot \boldsymbol{\mu} - \tau c(\tau), \\ \lambda_2(\mathbf{U}; \boldsymbol{\mu}) &= \dots = \lambda_{d+1}(\mathbf{U}; \boldsymbol{\mu}) = \mathbf{v} \cdot \boldsymbol{\mu}, \\ \lambda_{d+2}(\mathbf{U}; \boldsymbol{\mu}) &= \mathbf{v} \cdot \boldsymbol{\mu} + \tau c(\tau).\end{aligned}$$

Here $c(\tau) := \sqrt{p'(\tau)}$ is the speed of sound. As a consequence $\mathbf{U} \in (\tilde{\mathcal{A}}_{\text{liq}} \cup \tilde{\mathcal{A}}_{\text{vap}}) \times \mathbb{R}^d$ is a necessary (and in fact sufficient) criterion for (1) to be hyperbolic. For hyperbolic systems the notion of weak entropy solutions is widely believed to be the correct solution concept. Thus we search for functions $\mathbf{U} = \mathbf{U}(\mathbf{x}, t)$ which are weak solutions with $\varrho(\mathbf{x}, t) \in \tilde{\mathcal{A}}_{\text{liq/vap}}$ for almost all $(\mathbf{x}, t) \in \Omega_{\text{liq/vap}}(t) \times [0, T]$ and satisfy the entropy condition

$$E(\varrho, \mathbf{m})_t + \text{div}((E(\varrho, \mathbf{m}) + \tilde{p}(\varrho)) \mathbf{v}) \leq 0$$

in the distributional sense in the single bulk regions (not in the complete domain Ω where we have to take into account the surface energy, see (14) below). Here we used $E(\varrho, \mathbf{m}) = \varrho \psi(\varrho^{-1}) + \frac{|\mathbf{m}|^2}{2\varrho}$, $\mathbf{m} = \varrho \mathbf{v}$. It is straightforward to check that E is convex for states in the bulk sets and thus an entropy for (1).

To close the model (1) it remains to provide coupling conditions at the free boundary $\Gamma(t)$. For $\boldsymbol{\xi} \in \Gamma(t)$ let us denote the speed of $\Gamma(t)$ in the normal direction $\boldsymbol{\nu} = \boldsymbol{\nu}(\boldsymbol{\xi}, t) \in \mathbb{S}^{d-1}$ by $s = s(\boldsymbol{\xi}, t) \in \mathbb{R}$. The normal vector is always chosen as pointing into the vapor domain $\Omega_{\text{vap}}(t)$. Across the interface the following $d+1$ trace conditions which represent the conservation of mass and the balance of momentum in presence of capillary surface forces are posed.

$$[[\varrho(\mathbf{v} \cdot \boldsymbol{\nu} - s)]] = 0, \quad (6)$$

$$[[\varrho(\mathbf{v} \cdot \boldsymbol{\nu} - s) \mathbf{v} \cdot \boldsymbol{\nu} + \tilde{p}(\varrho)]] = (d-1) \zeta \kappa, \quad (7)$$

$$[[\mathbf{v} \cdot \mathbf{t}^l]] = 0 \quad (l = 1, \dots, d-1). \quad (8)$$

Thereby $[[a]] := a_{\text{vap}} - a_{\text{liq}}$ and $a_{\text{vap/liq}} := \lim_{\varepsilon \rightarrow 0, \varepsilon > 0} a(\boldsymbol{\xi} \pm \varepsilon \boldsymbol{\nu})$ for some quantity a defined in $\Omega_{\text{vap}}(t) \cup \Omega_{\text{liq}}(t)$. In (7) by $\kappa = \kappa(\boldsymbol{\xi}, t) \in \mathbb{R}$ we denote the mean curvature of $\Gamma(t)$ associated with orientation given through the choice of the normal $\boldsymbol{\nu}$. The constant surface tension coefficient is $\zeta \geq 0$, and $\mathbf{t}^1, \dots, \mathbf{t}^{d-1} \in \mathbb{S}^{d-1}$ are a complete set of tangential vectors.

In this work we are interested in non-characteristic phase boundaries, which are subsonic. For a subsonic phase boundary the adjacent states $\mathbf{U}_{\text{vap/liq}}$ are such that the undercompressivity condition

$$|\varrho_{\text{liq}}(\mathbf{v}_{\text{liq}} \cdot \boldsymbol{\nu} - s)| = |\varrho_{\text{vap}}(\mathbf{v}_{\text{vap}} \cdot \boldsymbol{\nu} - s)| < \min\{c(\tau_{\text{liq}}), c(\tau_{\text{vap}})\} \quad (9)$$

holds. It is known (see e.g. [1, 19]) that well-posedness of the free boundary value problem for (1) requires an additional condition. One possible choice is yet another algebraic coupling condition of the general form

$$K(\tau_{\text{liq}}, \tau_{\text{vap}}, j) = 0. \quad (10)$$

In (10) we used the relative mass flux

$$j = \varrho_{\text{liq}}(\mathbf{v}_{\text{liq}} \cdot \boldsymbol{\nu} - s) = \varrho_{\text{vap}}(\mathbf{v}_{\text{vap}} \cdot \boldsymbol{\nu} - s).$$

Functions $K : \mathcal{A}_{\text{liq}} \times \mathcal{A}_{\text{vap}} \times \mathbb{R} \rightarrow \mathbb{R}$ are usually called kinetic relations. We refer for more mathematical background to [14]. In Section 2.2 below we discuss possible kinetic relations.

2.2 Kinetic Relations

In the literature kinetic relations have been suggested (see [1, 19]), which control the entropy dissipation explicitly. In terms of the general form (10) these are given by

$$\mathcal{K}(\tau_{\text{liq}}, \tau_{\text{vap}}, j) := \left[\mu(\tau) + \frac{1}{2} \tau^2 j^2 \right] + k(j) = 0. \quad (11)$$

In (11) the driving force $k : \mathbb{R} \rightarrow \mathbb{R}$ is a smooth function, that satisfies

$$k(j)j \geq 0. \quad (12)$$

Later on we use the simple choice

$$k(j) = cj, \quad c \geq 0. \quad (13)$$

The relation of (11) to entropy consistency can be seen as follows. Multiplying (11) by the mass flux j and applying (6), (7) one obtains

$$-s (\llbracket E(\varrho, \mathbf{m}) \rrbracket) + (d-1) \zeta \kappa + \llbracket (E(\varrho, \mathbf{m}) + \tilde{p}(\varrho)) \mathbf{v} \cdot \boldsymbol{\nu} \rrbracket = -k(j)j. \quad (14)$$

This is nothing but the standard entropy jump conditions with an additional term for the interfacial energy. Condition (12) ensures that the entropy is dissipated.

We emphasize that the conditions (6), (7) and (11) agree with standard conditions for static two-phase equilibria.

Remark 2.1. Consider a spherical bubble or droplet at rest. For a bubble radius $r > 0$ the mean curvature is $\kappa = 1/r$ ($\kappa = -1/r$ for a droplet). The standard theory then requires [2] that the Young-Laplace law holds and the chemical potential is continuous across the interface, respectively given by

$$p(\tau_{\text{vap}}) - p(\tau_{\text{liq}}) = (d-1)\zeta/r \quad \text{and} \quad \mu(\tau_{\text{vap}}) = \mu(\tau_{\text{liq}}). \quad (15)$$

Our choice of the kinetic relation (11) includes such situations as stationary solutions, i.e., for $j = 0$.

For vanishing surface tension the conditions are known as the Maxwell equal-area rule. Then we have $p^* := p(\tau_{\text{liq}}) = p(\tau_{\text{vap}})$ and in view of (4) $0 = \mu(\tau_{\text{liq}}) - \mu(\tau_{\text{vap}}) = p^*(\tau_{\text{liq}} - \tau_{\text{vap}}) - \int_{\tau_{\text{liq}}}^{\tau_{\text{vap}}} p(\tau) d\tau$. It is important to note that the choice (5) puts some restrictions to subsonic phase boundaries (see (9)). For a subsonic phase boundary the graph of the line connecting τ_{liq} and τ_{vap} must intersect the graph of p in the interval $(\tau_{\text{liq}}^{\text{spinod}}, \tau_{\text{vap}}^{\text{spinod}})$. Thus the absolute pressure difference is bounded. For $r \ll 1$ this is obviously not possible and we do not have stationary solutions with $j = 0$. However, there are still admissible (dynamical) solutions with $j \neq 0$.

The observed non-existence of such stationary solutions is important for the relaxation approach in Section 3.

We consider in this paper a second kinetic relation which is often used in the literature (see e.g. [15, 18]). This kinetic relation does not depend on the relative flux j and without further conditions it is not clear whether an entropy statement like (14) holds. However its simpler structure makes it accessible for rigorous analysis. This kinetic relation $\mathbb{K} : \mathcal{A}_{\text{liq}} \times \mathcal{A}_{\text{vap}} \rightarrow \mathbb{R}$ is given by

$$\mathbb{K}(\tau_{\text{liq}}, \tau_{\text{vap}}) := \tau_{\text{vap}} - \varphi(\tau_{\text{liq}}). \quad (16)$$

The function $\varphi : \mathcal{A}_{\text{liq}} \rightarrow \mathcal{A}_{\text{vap}}$ is only assumed to be smooth and strictly monotone decreasing.

3 A Two-Phase Relaxation Riemann Solver

In this section we will introduce a relaxation approach for two-phase Riemann problems which is needed as microscale solver in the overall HMM in Section 4 below. The approach relies on [3, 4]. We will first describe the structure of the relaxation approximation and will then discuss the wellposedness of the approximative solution depending on the selected kinetic relation.

3.1 The Basic Structure of the Relaxation Approximation

As we will see in Section 4 the HMM provides for any point of the discrete interface states as input data for the microscale solver states $\mathbf{U}_{\text{Liq}} \in \mathcal{U}_{\text{liq}} := \tilde{\mathcal{A}}_{\text{liq}} \times \mathbb{R}^d$, $\mathbf{U}_{\text{Vap}} \in \mathcal{U}_{\text{vap}} := \tilde{\mathcal{A}}_{\text{vap}} \times \mathbb{R}^d$, an orthonormal system $\boldsymbol{\nu}, \mathbf{t}^1, \dots, \mathbf{t}^{d-1} \in \mathbb{S}^{d-1}$, and an associated (constant) curvature value $\kappa \in \mathbb{R}$. With the Riemann solver we compute then interfacial bulk states which result from the local interaction of the input data based on a chosen kinetic relation K . From the technical point of view the output of this section will be mappings of type

$$M_K : \begin{cases} \mathcal{U}_{\text{liq}} \times \mathcal{U}_{\text{vap}} \times (\mathbb{S}^{d-1})^d \times \mathbb{R} & \rightarrow \mathcal{U}_{\text{liq}} \times \mathcal{U}_{\text{vap}} \times \mathbb{R} \\ (\mathbf{U}_{\text{Liq}}, \mathbf{U}_{\text{Vap}}, \boldsymbol{\nu}, \mathbf{t}^1, \dots, \mathbf{t}^{d-1}, \kappa) & \mapsto (\mathbf{U}_{\text{liq}}, \mathbf{U}_{\text{vap}}, s). \end{cases} \quad (17)$$

The Riemann problem under consideration is now

$$\begin{pmatrix} \varrho \\ \varrho v \\ \varrho \mathbf{u} \end{pmatrix}_t + \begin{pmatrix} \varrho v \\ \varrho v^2 + \tilde{p}(\varrho) \\ \varrho v \mathbf{u} \end{pmatrix}_x = \begin{pmatrix} 0 \\ 0 \\ \mathbf{0} \end{pmatrix}, \quad (18)$$

for $x := \mathbf{x} \cdot \boldsymbol{\nu}$, $v := \mathbf{v} \cdot \boldsymbol{\nu}$ and $\mathbf{u} := (\mathbf{v} \cdot \mathbf{t}^1, \dots, \mathbf{v} \cdot \mathbf{t}^{d-1})^t$. It is subject to the initial condition

$$\begin{pmatrix} \varrho \\ v \end{pmatrix}(x, 0) = \begin{cases} (\varrho_{\text{Liq}}, \mathbf{v}_{\text{Liq}} \cdot \boldsymbol{\nu}, \mathbf{v}_{\text{Liq}} \cdot \mathbf{t}^1, \dots, \mathbf{v}_{\text{Liq}} \cdot \mathbf{t}^{d-1})^t & : x < 0, \\ (\varrho_{\text{Vap}}, \mathbf{v}_{\text{Vap}} \cdot \boldsymbol{\nu}, \mathbf{v}_{\text{Vap}} \cdot \mathbf{t}^1, \dots, \mathbf{v}_{\text{Vap}} \cdot \mathbf{t}^{d-1})^t & : x > 0. \end{cases} \quad (19)$$

We expect that the solution of this two-phase Riemann problem consists of $d+2$ waves, one wave being an undercompressive phase boundary with adjacent states $\mathbf{U}_{\text{liq}}, \mathbf{U}_{\text{vap}}$, see Figure 2 for some illustration. Exact Riemann solvers of this type can be found in [12, 15]. Note however that they do not cover the general kinetic relation (11) and surface tension.

For the reasons outlined in the introduction we approximate now the exact solution of (19) by the solution of the Riemann problem for a larger but more simple system. Precisely we solve the relaxation Riemann problem

$$\mathbf{V}_t + \mathbf{G}(\mathbf{V})_x = 0 \Leftrightarrow \begin{pmatrix} \varrho \\ \varrho v \\ \varrho \mathbf{u} \\ \varrho \pi \end{pmatrix}_t + \begin{pmatrix} \varrho v \\ \varrho v^2 + \pi \\ \varrho v \mathbf{u} \\ (\varrho \pi + a^2)v \end{pmatrix}_x = \begin{pmatrix} 0 \\ 0 \\ \mathbf{0} \\ 0 \end{pmatrix}, \quad (20)$$

subject to the initial datum

$$\mathbf{V}(x, 0) = \begin{cases} \mathbf{V}_{\text{Liq}} : x < 0, \\ \mathbf{V}_{\text{Vap}} : x > 0, \end{cases} \quad (21)$$

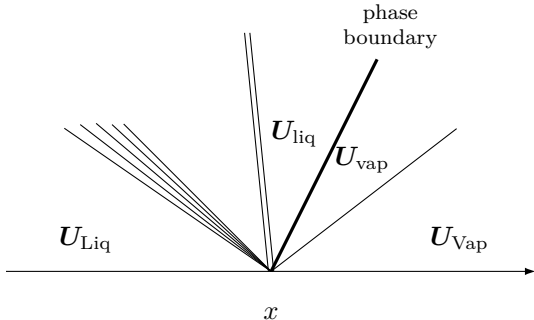


Figure 2: Typical wave structure for the exact two-phase Riemann problem.

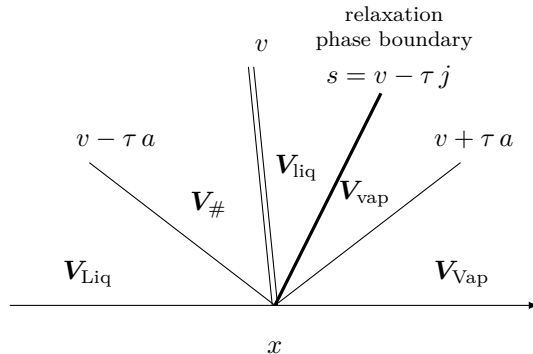


Figure 3: Typical wave fan of the approximated two-phase Riemann solution.

with

$$\begin{aligned} \mathbf{V}_{\text{Liq}} &= \varrho_{\text{Liq}} \left(1, \mathbf{v}_{\text{Liq}} \cdot \boldsymbol{\nu}, \mathbf{v}_{\text{Liq}} \cdot \mathbf{t}^1, \dots, \mathbf{v}_{\text{Liq}} \cdot \mathbf{t}^{d-1}, p(\tau_{\text{Liq}}) \right)^t, \\ \mathbf{V}_{\text{Vap}} &= \varrho_{\text{Vap}} \left(1, \mathbf{v}_{\text{Vap}} \cdot \boldsymbol{\nu}, \mathbf{v}_{\text{Vap}} \cdot \mathbf{t}^1, \dots, \mathbf{v}_{\text{Vap}} \cdot \mathbf{t}^{d-1}, p(\tau_{\text{Vap}}) \right)^t. \end{aligned}$$

The parameter $a > 0$ will be defined below. It is straightforward to see that (20) is hyperbolic in the convex state space $(0, b^{-1}) \times \mathbb{R}^{d+1}$. The eigenvalues of the Jacobian of \mathbf{G} are

$$\lambda_1^R(\mathbf{V}) = v - \tau a, \lambda_2^R(\mathbf{V}) = \dots = \lambda_{d+1}^R(\mathbf{V}) = v, \lambda_{d+2}^R(\mathbf{V}) = v + \tau a.$$

It is also readily checked that all characteristic fields of (20) are linear degenerate. Therefore the weak solution of (20), (21) with $a > 0$ is uniquely determined and made up of $d + 2$ contact discontinuities. This procedure would only provide a good approximation for one-phase problems. Because we want to solve a two-phase problem for some given kinetic relation $K : \mathcal{A}_{\text{liq}} \times \mathcal{A}_{\text{vap}} \times \mathbb{R} \rightarrow \mathbb{R}$, we will rely the approximation on a different wave fan (, which in general is not a weak solution of (20)). We propose to approximate the two-phase Riemann problem by adding an additional phase boundary (see Figure 3). This artificial phase boundary is a discontinuous wave that is supposed to satisfy the jump conditions

$$\begin{aligned} \dot{j} \llbracket \tau \rrbracket + \llbracket v \rrbracket &= 0, \quad \dot{j} \llbracket v \rrbracket + \llbracket \pi \rrbracket = C := (d-1) \zeta \kappa, \\ \llbracket \mathbf{u} \rrbracket &= 0, \quad K(\tau_{\text{liq}}, \tau_{\text{vap}}, \dot{j}) = 0. \end{aligned} \tag{22}$$

In this way we ensure that later on the jump conditions (6), (7), (8) and the kinetic relation (10) are preserved for the approximation (at least for fixed surface tension $C \in \mathbb{R}$). The number $\dot{j} = \dot{j}(\mathbf{V}_{\text{Liq}}, \mathbf{V}_{\text{Vap}})$ is a function of the states $\mathbf{V}_{\text{Liq}}, \mathbf{V}_{\text{Vap}}$, and a-priori not known exactly. We assume that this mapping satisfies

$$\dot{j} = \dot{j}(\mathbf{V}_{\text{Liq}}, \mathbf{V}_{\text{Vap}}) \in \mathcal{C}(\tilde{\mathcal{A}}_{\text{liq}} \times \mathbb{R}^{d+1} \times \tilde{\mathcal{A}}_{\text{vap}} \times \mathbb{R}^{d+1}). \tag{23}$$

All other waves are kept satisfying the standard Rankine-Hugoniot conditions. Such an approach was introduced in [3] for the p -system.

Let now some \dot{j} be given and assume that \dot{j} does not vanish. W.l.o.g. we consider $\dot{j} < 0$. This implies for any $\mathbf{V} \in (0, b^{-1}) \times \mathbb{R}^{d+1}$

$$\lambda_2^R(\mathbf{V}) = \dots = \lambda_{d+1}^R(\mathbf{V}) = v < v - \tau \dot{j}.$$

The case $\dot{j} > 0$ can be treated in an analogous way, for $\dot{j} = 0$ see Remark 3.4.

Now we let $a > -\dot{j}$ and search for a function $\mathbf{V} : \mathbb{R} \times (0, T) \rightarrow (\tilde{\mathcal{A}}_{\text{liq}} \cup \tilde{\mathcal{A}}_{\text{vap}}) \times \mathbb{R}^{d+1}$ given by

$$\mathbf{V}(x, t) = \begin{pmatrix} \varrho \\ \varrho v \\ \varrho \mathbf{u} \\ \varrho \pi \end{pmatrix} = \begin{cases} \mathbf{V}_{\text{Liq}} & \text{for } x \leq t\sigma_1, \\ \mathbf{V}_{\#} & \text{for } t\sigma_1 > x \leq t\sigma_2, \\ \mathbf{V}_{\text{liq}} & \text{for } t\sigma_2 > x \leq t\sigma_3, \\ \mathbf{V}_{\text{vap}} & \text{for } t\sigma_3 > x \leq t\sigma_4, \\ \mathbf{V}_{\text{vap}} & \text{for } t\sigma_4 > x \end{cases} \quad (24)$$

with propagation speeds

$$\begin{aligned} \sigma_1 &= \lambda_1^R(\mathbf{V}_1) = \lambda_1^R(\mathbf{V}_{\#}), & \sigma_2 &= \lambda_2^R(\mathbf{V}_{\#}) = \lambda_2^R(\mathbf{V}_{\text{liq}}), \\ \sigma_3 &= s, & \sigma_4 &= \lambda_{d+2}^R(\mathbf{V}_{\text{vap}}) = \lambda_{d+2}^R(\mathbf{V}_r). \end{aligned}$$

The states \mathbf{V}_{liq} and \mathbf{V}_{vap} are connected by a discontinuity which we call *relaxation phase boundary*. From $a > -\dot{j} > 0$ we see immediately that the ordering of the waves in (24) is consistent. For the case $\dot{j} > 0$ the relaxation phase boundary would move slower than the contact wave and the construction (24) has to be changed accordingly.

We summarize the conditions for the three unknown intermediate states $\mathbf{V}_{\#}$, \mathbf{V}_{liq} and \mathbf{V}_{vap} in (24) in Table 1. The obviously redundant relations are already skipped. Altogether we obtain 11 linear equations and one nonlinear equation for twelve unknowns. Note that we use the $[[\cdot]]$ -notation not only for the (relaxation) phase boundary but for all discontinuities. We call a function \mathbf{V} of form (24) *relaxation approximation for the kinetic relation K* if all conditions from Table 1 are satisfied. The solution of this algebraic problem depends on the choice of the kinetic relation and will be investigated in the next section.

$[[\mathbf{V}]] := \mathbf{V}_{\#} - \mathbf{V}_{\text{Liq}}$	$[[\mathbf{V}]] := \mathbf{V}_{\text{liq}} - \mathbf{V}_{\#}$	$[[\mathbf{V}]] := \mathbf{V}_{\text{vap}} - \mathbf{V}_{\text{liq}}$	$[[\mathbf{V}]] := \mathbf{V}_{\text{vap}} - \mathbf{V}_{\text{vap}}$
$\sigma_1 = v - \tau a$	$\sigma_2 = v$	$\sigma_3 = v - \tau \dot{j}$	$\sigma_4 = v + \tau a$
$-a [[\tau]] + [[v]] = 0$	$[[v]] = 0$	$-\dot{j} [[\tau]] + [[v]] = 0$	$a [[\tau]] + [[v]] = 0$
$a [[v]] + [[\pi]] = 0$	$[[\pi]] = 0$	$\dot{j} [[v]] + [[\pi]] = C$	$-a [[v]] + [[\pi]] = 0$
$[[\mathbf{u}]] = 0$		$[[\mathbf{u}]] = 0$	$[[\mathbf{u}]] = 0$
		$K(\tau_{\text{liq}}, \tau_{\text{vap}}, \dot{j}) = 0$	

Table 1: Jump conditions for the two-phase relaxation Riemann problem. Each column stands for one wave in the representation formula (24).

3.2 Wellposednes of the Two-Phase Relaxation Riemann Solver

The main results of this section are Theorems 3.1 and 3.2 which give existence, uniqueness, and continuous dependence statements for the kinetic relations \mathbb{K} from (16) and \mathcal{K} from (11), respectively.

Theorem 3.1. *Consider the kinetic relation \mathbb{K} from (16) and let $(\mathbf{U}_{\text{Liq}}, \mathbf{U}_{\text{vap}}, \boldsymbol{\nu}, \mathbf{t}^1, \dots, \mathbf{t}^{d-1}, \kappa) \in \mathcal{U}_{\text{liq}} \times \mathcal{U}_{\text{vap}} \times (\mathbb{S}^{d-1})^d \times \mathbb{R}$ of function $M_{\mathbb{K}}$ from (17) be given such that $\dot{j} < 0$ holds.*

Then there exists a positive number \bar{a} such that for all $a > \bar{a}$ there is a unique relaxation approximation \mathbf{V} for \mathbb{K} . In particular \mathbf{V} satisfies $\varrho_{\#}, \varrho_{\text{liq}} \in \tilde{\mathcal{A}}_{\text{liq}}$ and $\varrho_{\text{vap}} \in \tilde{\mathcal{A}}_{\text{vap}}$.

The mapping $M_{\mathbb{K}}$ is continuous.

Proof. The proof is given for the case $\dot{j}(\mathbf{V}_{\text{Liq}}, \mathbf{V}_{\text{vap}}) < 0$, the positive case is similar. First we show that the system of 12 equations from Table 1 is uniquely solvable. Choose \bar{a} such that $\dot{j} \in (-\bar{a}, 0)$ holds which is possible due to (23). Using all jump conditions except the kinetic

relation a straightforward computation shows that all unknowns can be expressed in terms of $\tau := \tau_{\text{liq}}$. In particular we have for $a > \bar{a}$ the relation $\tau_{\text{vap}} = A^a \tau + B^a$ with

$$\begin{aligned} A^a &= A^a(\mathbf{V}_{\text{Liq}}, \mathbf{V}_{\text{Vap}}) = \frac{a \dot{j} - \dot{j}^2}{2a^2 + a \dot{j} - \dot{j}^2}, \\ B^a &= B^a(\mathbf{V}_{\text{Liq}}, \mathbf{V}_{\text{Vap}}) = \frac{\pi_{\text{Vap}} - \pi_{\text{Liq}} + a(v_{\text{Vap}} - v_{\text{Liq}}) + 2a^2 \tau_{\text{Vap}} - C}{2a^2 + a \dot{j} - \dot{j}^2}. \end{aligned} \quad (25)$$

To conclude we define the mapping $F_a : \mathcal{A}_{\text{liq}} \rightarrow \mathbb{R}$ by $F_a(\tau) = \varphi^{-1}(A^a \tau + B^a)$. Recall that φ is strictly decreasing and $\varphi^{-1} : \mathcal{A}_{\text{vap}} \rightarrow \mathcal{A}_{\text{liq}}$ exists. Furthermore we have $A^a \rightarrow 0$ and $B^a \rightarrow \tau_{\text{vap}} \in \mathcal{A}_{\text{vap}}$ for $a \rightarrow \infty$. Thus $A^a \tau + B^a \in \mathcal{A}_{\text{vap}}$ for all τ in the bounded set \mathcal{A}_{liq} for $a > \bar{a}$, possibly increasing once more \bar{a} . Again using $A^a \rightarrow 0$ we observe that F_a is contracting since φ is smooth. Thus there exists a unique solution of the equations from Table 1, the corresponding mapping $M_{\mathbb{K}}$ is continuous.

There is a continuous function $g = g(\mathbf{V}_{\text{Liq}}, \mathbf{V}_{\text{Vap}}, a)$ with $g(\mathbf{V}_{\text{Liq}}, \mathbf{V}_{\text{Vap}}, a) \rightarrow 0$ for $a \rightarrow \infty$ such that $\tau_{\#} = \tau_{\text{Liq}} + g(\mathbf{V}_{\text{Liq}}, \mathbf{V}_{\text{Vap}}, a)$ holds. Then we find $\tau_{\#} \in \mathcal{A}_{\text{liq}}$ for sufficiently large \bar{a} . \square

Theorem 3.1 gives a global existence result. For the more realistic kinetic relation \mathcal{K} from (11) we are only able to show a result for initial datum close to states which produce a single phase boundary as traveling wave solution.

Precisely consider $(\hat{\mathbf{U}}_{\text{Liq}}, \hat{\mathbf{U}}_{\text{Vap}}, \hat{\boldsymbol{\nu}}, \hat{\mathbf{t}}^1, \dots, \hat{\mathbf{t}}^{d-1}, \hat{\kappa}) \in \tilde{\mathcal{A}}_{\text{liq}} \times \mathbb{R}^d \times \tilde{\mathcal{A}}_{\text{vap}} \times \mathbb{R}^d \times (\mathbb{S}^{d-1})^d \times \mathbb{R}$ and a number $\hat{j} < 0$ that satisfy

$$\begin{aligned} -\hat{j}(\hat{\tau}_{\text{Vap}} - \hat{\tau}_{\text{Liq}}) + (\hat{v}_{\text{Vap}} - \hat{v}_{\text{Liq}}) &= 0, \\ \hat{j}(\hat{v}_{\text{Vap}} - \hat{v}_{\text{Liq}}) + p(\hat{\tau}_{\text{Vap}}) - p(\hat{\tau}_{\text{Liq}}) &= (d-1) \zeta \hat{\kappa}, \\ \hat{\mathbf{u}}_{\text{Liq}} - \hat{\mathbf{u}}_{\text{Vap}} = 0, \quad \mathcal{K}(\hat{\tau}_{\text{Liq}}, \hat{\tau}_{\text{Vap}}, \hat{j}) &= 0. \end{aligned} \quad (26)$$

Then

$$\hat{\mathbf{U}}(x, t) = \hat{\mathbf{U}}_{\text{Liq}} \text{ for } x - \hat{s}t < 0 \text{ and } \hat{\mathbf{U}}(x, t) = \hat{\mathbf{U}}_{\text{Vap}} \text{ for } x - \hat{s}t > 0 \quad (27)$$

is a single phase boundary that is a solution of (18), (19) with speed $\hat{s} = \hat{v}_{\text{Liq}} - \hat{\tau}_{\text{Liq}} \hat{j} > 0$.

Due to (22) the single relaxation phase boundary

$$\hat{\mathbf{V}}(x, t) = \hat{\mathbf{V}}_{\text{Liq}} \text{ for } x - \hat{s}t < 0 \text{ and } \hat{\mathbf{V}}(x, t) = \hat{\mathbf{V}}_{\text{Vap}} \text{ for } x - \hat{s}t > 0 \quad (28)$$

is also a relaxation approximation when $\dot{j} = \hat{j}$ holds.

Theorem 3.2. *For a kinetic relation \mathcal{K} let $(\hat{\mathbf{U}}_{\text{Liq}}, \hat{\mathbf{U}}_{\text{Vap}}, \hat{\boldsymbol{\nu}}, \hat{\mathbf{t}}^1, \dots, \hat{\mathbf{t}}^{d-1}, \hat{\kappa}, \hat{j})$ from (27) be given such that $\hat{j}(\hat{\mathbf{V}}_{\text{Liq}}, \hat{\mathbf{V}}_{\text{Vap}}) \neq 0$ and the conditions*

$$|\hat{j}| < \max \{ c(\hat{\tau}_{\text{Liq}}), c(\hat{\tau}_{\text{Vap}}) \} \quad \text{and} \quad \hat{j}(\hat{\mathbf{V}}_{\text{Liq}}, \hat{\mathbf{V}}_{\text{Vap}}) = \hat{j} \quad (29)$$

hold.

Then there exists a number $\bar{a} > 0$ and an open set $\mathcal{W} \subset \mathcal{U}_{\text{liq}} \times \mathcal{U}_{\text{vap}} \times (\mathbb{S}^{d-1})^d \times \mathbb{R}$ with $(\hat{\mathbf{U}}_{\text{Liq}}, \hat{\mathbf{U}}_{\text{Vap}}, \hat{\boldsymbol{\nu}}, \hat{\mathbf{t}}^1, \dots, \hat{\mathbf{t}}^{d-1}, \hat{\kappa}) \in \mathcal{W}$ such that there is for all $(\mathbf{U}_{\text{Liq}}, \mathbf{U}_{\text{Vap}}, \boldsymbol{\nu}, \mathbf{t}^1, \dots, \mathbf{t}^{d-1}, \kappa) \in \mathcal{W}$ and all $a > \bar{a}$ a unique relaxation approximation \mathbf{V} for \mathcal{K} . In particular \mathbf{V} satisfies $\varrho_{\#}, \varrho_{\text{liq}} \in \tilde{\mathcal{A}}_{\text{liq}}$ and $\varrho_{\text{vap}} \in \tilde{\mathcal{A}}_{\text{vap}}$.

The mapping $M_{\mathcal{K}}$ from (17) is continuous.

Remark 3.3. The first condition in (29) renders the single phase boundary (27) to be a subsonic wave. It is included in the defining relation (9).

Proof of Theorem 3.2. We present the proof for the case $\hat{j}(\hat{\mathbf{V}}_{\text{Liq}}, \hat{\mathbf{V}}_{\text{Vap}}) < 0$. As in the proof of Theorem 3.1 we condense the conditions in Table 1 to a scalar equation for τ_{vap} in terms of $\tau = \tau_{\text{liq}}$. One finds for $T_a(\tau) = T_a(\tau; \mathbf{V}_{\text{Liq}}, \mathbf{V}_{\text{Vap}}) := A^a(\mathbf{V}_{\text{Liq}}, \mathbf{V}_{\text{Vap}})\tau + B^a(\mathbf{V}_{\text{Liq}}, \mathbf{V}_{\text{Vap}})$ again the relation

$$\tau_{\text{vap}} = T_a(\tau_{\text{liq}}; \mathbf{V}_{\text{Liq}}, \mathbf{V}_{\text{Vap}}),$$

where A^a and B^a are defined as in (25). Applying the kinetic relation (11) we can eliminate τ_{vap} and obtain the scalar equation

$$F_a(\tau) = F_a(\tau; \mathbf{V}_{\text{Liq}}, \mathbf{V}_{\text{Vap}}) := \mathcal{K}(\tau, T_a(\tau; \mathbf{V}_{\text{Liq}}, \mathbf{V}_{\text{Vap}}), \dot{j}(\mathbf{V}_{\text{Liq}}, \mathbf{V}_{\text{Vap}})) = 0,$$

or writing out \mathcal{K}

$$\mu(T_a(\tau; \mathbf{V}_{\text{Liq}}, \mathbf{V}_{\text{Vap}})) - \mu(\tau) + \frac{\dot{j}^2}{2} (T_a(\tau; \mathbf{V}_{\text{Liq}}, \mathbf{V}_{\text{Vap}})^2 - \tau^2) + k(\dot{j}) = 0.$$

As in the proof of Theorem 3.1 we see that $F_a : \mathcal{A}_{\text{liq}} \rightarrow \mathbb{R}$ is well-defined for a sufficiently large. We know from (26) that $T_a(\hat{\tau}_{\text{Liq}}; \hat{\mathbf{V}}_{\text{Liq}}, \hat{\mathbf{V}}_{\text{Vap}}) = \hat{\tau}_{\text{Vap}}$ and thus

$$F_a(\hat{\tau}_{\text{Liq}}; \hat{\mathbf{V}}_{\text{Liq}}, \hat{\mathbf{V}}_{\text{Vap}}) = 0 \tag{30}$$

holds with (29).

Now, recall from (4) that the chemical potential satisfies $\mu'(\tau) = \tau p'(\tau)$. Then the derivative of F_a with respect to τ is

$$\begin{aligned} F'_a(\tau) &= T_a(\tau) p'(T_a(\tau)) T'_a(\tau) - \tau p'(\tau) + \dot{j}^2 (T_a(\tau) T'_a(\tau) - \tau) \\ &= \tau (-p'(\tau) - \dot{j}^2) - T_a(\tau) T'_a(\tau) (-p'(T_a(\tau)) - \dot{j}^2). \end{aligned}$$

From (29) we conclude $p'(\hat{\tau}_{\text{Liq}/\text{Vap}}) + \dot{j}^2 = -c^2(\hat{\tau}_{\text{Liq}/\text{Vap}}) + \hat{j}^2 < 0$. Moreover we can choose \bar{a} such that the relation $T_a(\hat{\tau}_{\text{Liq}}; \hat{\mathbf{V}}_{\text{Liq}}, \hat{\mathbf{V}}_{\text{Vap}}) A_a(\hat{\mathbf{V}}_{\text{Liq}}, \hat{\mathbf{V}}_{\text{Vap}}) < 0$ holds for all $a > \bar{a}$, such that we get

$$F'_a(\hat{\tau}_{\text{Liq}}; \hat{\mathbf{V}}_{\text{Liq}}, \hat{\mathbf{V}}_{\text{Vap}}) > 0.$$

Then we can deduce from (30) that there exists at least locally a unique relaxation approximation \mathbf{V} for \mathcal{K} such that moreover $M_{\mathcal{K}}$ is continuous. \square

Remark 3.4. Theorem 3.2 is proven for the case that $\dot{j}(\mathbf{V}_{\text{Liq}}, \mathbf{V}_{\text{Vap}})$ does not vanish. The existence of a relaxation approximation can also be proven for the zero case provided the condition

$$\dot{j}(\mathbf{V}_{\text{Liq}}, \mathbf{V}_{\text{Vap}}) = 0 \Leftrightarrow \hat{\mathbf{V}} \text{ from (28) with } \mathbf{V}_{\text{Liq}/\text{Vap}} = \hat{\mathbf{V}}_{\text{Liq}/\text{Vap}}, \hat{j} = 0 \text{ solves (26)}$$

holds. Then (24) remains well-defined since then $\mathbf{V}_{\#} = \mathbf{V}_{\text{liq}}$ holds.

4 A Heterogeneous Multiscale Method for Radially Symmetric Solutions

In this section we present our numerical approach to solve the free boundary value problem (1), (2), (3) with a phase boundary that obeys (6), (7), (8) and (10). For other numerical methods for undercompressive waves in systems of conservation laws for two-phase flow we refer to [6, 7, 18, 21]. We will restrict ourselves to the onedimensional case $d = 1$ and radially symmetric solutions in \mathbb{R}^d for $d > 1$. In this way it is possible to take into account curvature effects without being in need for a complex computation of the curvature.

Let us introduce first the transformed setting [16]. For $R_{\text{max}} > R_{\text{min}} > 0$ let $\mathbf{U} = \mathbf{U}(\mathbf{x}, t) = (\varrho(\mathbf{x}, t), \mathbf{m}(\mathbf{x}, t)^t)^t$ be a radially symmetric solution of the system (1) in $\Omega \times [0, T]$ with $\Omega = \{\mathbf{x} \in \mathbb{R}^d \mid R_{\text{min}} < |\mathbf{x}| < R_{\text{max}}\}$. We assume that there is a single interface of form $\Gamma(t) = \gamma(t) \mathbb{S}^{d-1}$ with $\gamma(t) \in (R_{\text{min}}, R_{\text{max}})$ for $t \in [0, T]$. Then there is (accepting a double use of notations for the density) a function $\mathbf{W} = \mathbf{W}(r, t) = (\varrho(r, t), m(r, t))^t$ with

$$\varrho(\mathbf{x}, t) = \varrho(r, t), \quad \mathbf{m}(\mathbf{x}, t) = \frac{\mathbf{x}}{r} m(r, t), \quad |\mathbf{x}| = r. \tag{31}$$

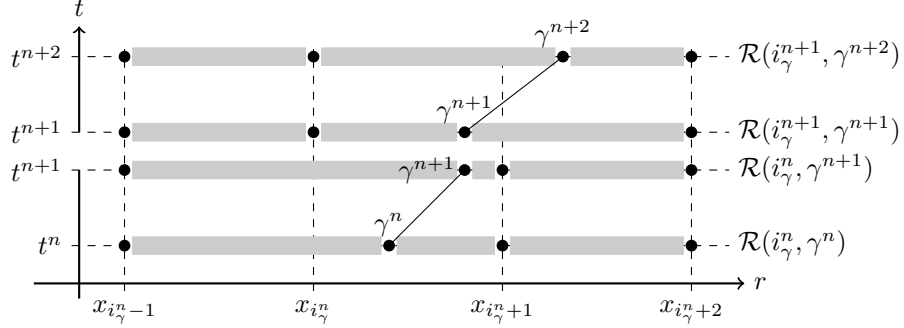


Figure 4: Possible mesh modification: moving mesh strategy for $t^n \rightarrow t^{n+1}$ resp. $t^{n+1} \rightarrow t^{n+2}$ and local remeshing when $i_\gamma^{n+1} = i_\gamma^n + 1$. The dots denote the actual partition obtained by applying \mathcal{R} and the grey boxes indicate the cells.

$\mathbf{W} : ((R_{\min}, R_{\max}) \setminus \gamma(t)) \times [0, T) \rightarrow (\tilde{\mathcal{A}}_{\text{liq}} \cup \tilde{\mathcal{A}}_{\text{vap}}) \times \mathbb{R}$ satisfies

$$\mathbf{W}_t + \frac{1}{r^{d-1}} (r^{d-1} \mathbf{F}(\mathbf{W}))_r = \frac{d-1}{r^{d-1}} \mathbf{Q}(\mathbf{W}) \quad (32)$$

in $\{(r, t) \in (R_{\min}, R_{\max}) \times (0, T) \mid r \neq \gamma(t)\}$. In view of (2), (3) the system (32) is completed with the initial condition

$$\mathbf{W}(r, 0) = \mathbf{W}_0(r) := \varrho_0(\mathbf{x}) (1, \mathbf{v}_0(\mathbf{x}) \cdot \mathbf{x})^t, \quad |\mathbf{x}| = r,$$

and $m(R_{\min}, t) = m(R_{\max}, t) = 0$ for $t \in [0, T)$. In (32) the functions $\mathbf{F}, \mathbf{Q} : (\tilde{\mathcal{A}}_{\text{liq}} \cup \tilde{\mathcal{A}}_{\text{vap}}) \times \mathbb{R} \rightarrow \mathbb{R}^2$ are given by

$$\mathbf{F}(\mathbf{W}) = \begin{pmatrix} m \\ \frac{m^2}{\varrho} + \tilde{p}(\varrho) \end{pmatrix}, \quad \mathbf{Q}(\mathbf{W}) = \begin{pmatrix} 0 \\ \tilde{p}(\varrho) \end{pmatrix}.$$

The macrosolver of the numerical scheme can be classified as a moving mesh finite volume scheme with explicit time stepping. For two successive time levels $t^n < t^{n+1}$, $n \in \mathbb{N}$, the associated time step is defined by $\Delta t^n = t^{n+1} - t^n$.

For the introduction to the moving mesh strategy let us introduce first the points $R_{\min} = x_0 < x_1 < \dots < x_{I+1} = R_{\max}$. The numerical algorithm will determine for any $n \in \mathbb{N}$ a number $\gamma^n \in (R_{\min}, R_{\max})$ which stands for the position of the discrete phase boundary at time t^n . Let

$$i_\gamma^n = \begin{cases} k & \text{if } |\gamma^n - x_k| < |\gamma^n - x_i| \text{ for all } i = 1, \dots, I, i \neq k, \\ i & \text{if } |\gamma^n - x_i| = |\gamma^n - x_{i+1}|. \end{cases} \quad (33)$$

the index of the closest point to γ^n . For the spatial discretization we introduce a time-dependent partition through the function $\mathcal{R} : \mathbb{N} \times \mathbb{R} \rightarrow \mathcal{P}(\mathbb{R})$,

$$\mathcal{R}(i_\gamma^n, \gamma^n) = \left\{ r_0, \dots, r_{I+1} \in [R_{\min}, R_{\max}] \mid r_i = x_i \text{ for } i \neq i_\gamma^n \text{ and } r_{i_\gamma^n} = \gamma^n \right\}.$$

Figure 4 shows possible realizations of \mathcal{R} .

In order to preserve the original multidimensional conservation we consider (32) not as a one-dimensional system, but approximate cell averages for the original spherically symmetric situation, see e.g. [17]. We follow then the classical finite volume strategy in \mathbb{R}^d instead and introduce multidimensional grid cells

$$K_i^n = \{ \mathbf{x} \in \mathbb{R}^d \mid r_i^n \leq |\mathbf{x}| \leq r_{i+1}^n \} \text{ for } r_i^n \in \mathcal{R}(i_\gamma^n, \gamma^n), \quad i = 0, \dots, I,$$

with cell volume $|K_i^n| = A_d(r_{i+1}^n) - A_d(r_i^n)$ and surface measure $|\partial K_i^n| = A'_d(r_{i+1}^n) - A'_d(r_i^n)$. Here $A_d(r)$ is the volume of a d -dimensional sphere with radius $r > 0$.

We consider now iterates

$$\mathbf{W}_i^n \approx \frac{1}{|K_i^n|} \int_{r_i^n}^{r_{i+1}^n} A'_d(r) \mathbf{W}(r, t^n) dr.$$

The family $\{ \mathbf{W}_i^n \mid n \in \mathbb{N}, 0 \leq i \leq I \}$ is computed for $i = 0, \dots, I$ by

$$|K_i^{n+1}| \mathbf{W}_i^{n+1} = |K_i^n| \mathbf{W}_i^n - \Delta t^n \left(A'_d(r_{i+1}^n) \mathbf{F}_{i+1,-}^n - A'_d(r_i^n) \mathbf{F}_{i,+}^n - (A'_d(r_{i+1}^n) - A'_d(r_i^n)) \mathbf{Q}(\mathbf{W}_i^n) \right) \quad (34)$$

for $n > 0$, K_i^{n+1} with respect to $\mathcal{R}(i_\gamma^n, \gamma^{n+1})$, and

$$\mathbf{W}_i^0 = \frac{1}{|K_i^0|} \int_{r_i^0}^{r_{i+1}^0} A'_d(r) \mathbf{W}_0(r) dr.$$

It remains to fix the fluxes $\mathbf{F}_{i,-/+}^n$ in (34). Let $\mathbf{F}_{\text{num}} : ((\tilde{\mathcal{A}}_{\text{liq}} \cup \tilde{\mathcal{A}}_{\text{vap}}) \times \mathbb{R})^2 \rightarrow \mathbb{R}^2$ be an arbitrary numerical flux that is consistent with \mathbf{F} from (32). In the numerical experiments we use the local Lax-Friedrichs flux. Furthermore we assume that we have for a given kinetic relation K a mapping M_K as in (17). We apply M_K (see (35) below) and get two states denoted by $\mathbf{W}_{-/+}^n$ and the speed denoted by s^n . The fluxes for (34) are then given by

$$\mathbf{F}_{i,-/+}^n = \begin{cases} \mathbf{F}_{\text{num}}(\mathbf{W}_{i-1}^n, \mathbf{W}_i^n) & \text{for } i \neq i_\gamma^n, \\ \mathbf{F}(\mathbf{W}_{-/+}^n) - s^n \mathbf{W}_{-/+}^n & \text{for } i = i_\gamma^n. \end{cases}$$

For given iterates $\{ \mathbf{W}_i^n \mid n \in \mathbb{N}, 0 \leq i \leq I \}$ we define the piecewise constant approximation

$$\mathbf{W}_h(r, t) = \mathbf{W}_i^n \text{ for } (r, t) \in [r_i^n, r_{i+1}^n) \times [t^n, t^{n+1}).$$

Remark 4.1. We stress that the scheme (34) can be understood as a moving mesh method or alternatively as a classical finite volume method on a space-time mesh. In Figure 4 we display the underlying mesh structure. For a scalar model problem we refer to [5] and for the case $d = 1$ to [8]. The moving mesh ansatz allows to define a mass conservative discretization.

We summarize the overall model in the subsequent algorithm which takes the form of a multi-scale method. To ease the notation assume that the initial data is in the liquid (vapour) state for $r < \gamma^0$ ($r > \gamma^0$) (droplet configuration).

Algorithm 4.2 (Heterogeneous multiscale method). *Let a kinetic relation K , an associated mapping M_K , $\mathbf{W}_0^0, \dots, \mathbf{W}_I^0$ and γ^0 be given. Find i_γ^0 via (33), construct $\mathcal{R}(i_\gamma^0, \gamma^0)$, and set $n = 0$, $s^0 = 0$.*

While $t^n < T$ **Do**

Step 1: Microscale. *Compute with $\mathbf{U}_{\text{Liq}} = ((\mathbf{W}_{i_\gamma^n}^n)^t, \mathbf{0})^t$,*

$$\mathbf{U}_{\text{Vap}} = ((\mathbf{W}_{i_\gamma^n}^n)^t, \mathbf{0})^t \text{ and } \mathbf{0} \in \mathbb{R}^{d-1}$$

$$(\mathbf{U}_{\text{liq}}, \mathbf{U}_{\text{vap}}, s^n) = M_K \left(\mathbf{U}_{\text{Liq}}, \mathbf{U}_{\text{Vap}}, \mathbf{e}^1, \dots, \mathbf{e}^d, \frac{1}{\gamma^n} \right), \quad (35)$$

where $\mathbf{e}^i \in \mathbb{R}^d$ is the i th unit vector. Define $\mathbf{W}_{-/+}^n = (\mathbf{U}_{\text{liq/vap}})_{1,2}$.

Step 2: Time Step. *The time step Δt^n is chosen according to a standard CFL condition in the bulk regions, and such that $2s^n \Delta t^n < (r_{i_\gamma^{n+1}} - \gamma^n)$ for $s^n > 0$ and $2s^n \Delta t^n < (r_{i_\gamma^{n-1}} - \gamma^n)$ for $s^n < 0$ holds. Put $t^{n+1} = t^n + \Delta t^n$, $\gamma^{n+1} = \gamma^n + s^n \Delta t^n$.*

Step 3: Macroscale. Construct the new mesh $\mathcal{R}(i_\gamma^n, \gamma^{n+1})$, compute $|K_i^{n+1}|$ and apply the update formula (34) for $i = 0, \dots, I$ to obtain $\mathbf{W}_h(\cdot, t^{n+1})$.

Step 4: Projection to New Mesh. Find i_γ^{n+1} according to (33). If $i_\gamma^{n+1} \neq i_\gamma^n$ the function $\mathbf{W}_h(\cdot, t^{n+1})$ is substituted by the L^2 -projection of itself onto the set of piecewise constant functions defined on $\mathcal{R}(i_\gamma^{n+1}, \gamma^{n+1})$.

Step 4: $n \mapsto n + 1$

Figure 4 illustrates the conservative projection step from $\mathcal{R}(i_\gamma^n, \gamma^{n+1})$ to $\mathcal{R}(i_\gamma^{n+1}, \gamma^{n+1})$. The proposed Algorithm 4.2 has the following properties:

Lemma 4.3. (i) The HMM 4.2 with (11) or (16) is mass conservative for $d \in \mathbb{N}$ and conserves momentum for $d = 1$.

(ii) Consider a single phase boundary (27) for \mathcal{K} and let $\hat{\mathbf{W}}_{\text{Liq}}$ and $\hat{\mathbf{W}}_{\text{Vap}}$ be the rotationally transformed states computed from (31).

- For $d = 1$ there holds

$$\mathbf{W}_i^n = \begin{cases} \hat{\mathbf{W}}_{\text{Liq}} & : i < i_\gamma^n, \\ \hat{\mathbf{W}}_{\text{Vap}} & : i \geq i_\gamma^n. \end{cases} \quad (36)$$

- If $d \geq 1$ and $\hat{v}_{\text{Liq}} = \hat{v}_{\text{Vap}} = \hat{s} = 0$ the initial configuration is preserved, i.e. (36) is valid with $i_\gamma^n = i_\gamma^0$ for all $n > 1$ (static phase boundary).

Up to our knowledge there is no simple fully conservative finite volume scheme for (32) with $d > 1$. Furthermore we can not expect (36) in the dynamic case. Constant functions are not maintained due to the intrinsic geometry change.

Proof. (i) For $d = 1$ the source term in (32) vanishes and $\mathbf{F}_{i_\gamma^n, -}^n = \mathbf{F}_{i_\gamma^n, +}^n$ holds. The volume integral over (34) gives

$$\sum_i |K_i^{n+1}| \mathbf{W}_i^{n+1} = \sum_i |K_i^n| \mathbf{W}_i^n - \Delta t^n \underbrace{\sum_i (A'_d(r_{i+1}^n) \mathbf{F}_{i+1, -}^n - A'_d(r_i^n) \mathbf{F}_{i, +}^n)}_{=0}.$$

With $d > 1$, the same argument holds for the first component of \mathbf{W} .

(ii) For $d = 1$ the source term vanishes and $\mathbf{F}_{i+1, -}^n = \mathbf{F}_{i, +}^n$ holds for $i \neq i_\gamma^n$. With (34) we obtain in the cell with index i_γ^n

$$(x_{i_\gamma^n+1} - \gamma^{n+1}) \mathbf{W}_{i_\gamma^n}^{n+1} = (x_{i_\gamma^n+1} - \gamma^n) \hat{\mathbf{W}}_{\text{Vap}} - \Delta t^n (\mathbf{F}(\hat{\mathbf{W}}_{\text{Vap}}) - \mathbf{F}(\hat{\mathbf{W}}_{\text{Vap}}) + \hat{s} \hat{\mathbf{W}}_{\text{Vap}}).$$

Since $\gamma^{n+1} = \gamma^n + s^n \Delta t^n$ we find $\mathbf{W}_{i_\gamma^n}^{n+1} = \hat{\mathbf{W}}_{\text{Vap}}$ and analogously $\mathbf{W}_{i_\gamma^n-1}^{n+1} = \hat{\mathbf{W}}_{\text{Liq}}$.

Let us now consider the case $d > 1$ where $m_i^n = s^n = 0$ holds. It is enough to consider the second component of (34). We have for $i = 0, \dots, I$

$$|K_i^{n+1}| m_i^{n+1} = |K_i^n| m_i^n - \Delta t^n (A'_d(r_{i+1}^n) \tilde{p}(\varrho_{i+1}^n) - A'_d(r_i^n) \tilde{p}(\varrho_i^n) - (A'_d(r_{i+1}^n) - A'_d(r_i^n)) \tilde{p}(\varrho_i^n)).$$

The pressure cancels out such that by $K^{n+1} = K^n$ due to $s^n = 0$ in all cells $m_i^{n+1} = m_i^n$ is satisfied. □

	γ^0	ϱ_l	ϱ_r	v_l	v_r	ζ	c	d
(a)	1	1.7	0.4	-0.2	-0.2	0	1	1
(b)	1	1.9	0.3	0	-0.2	0.1	1	2
(c)	1	1.9	0.3	-1	-1	0.1	1	2
(d)	1	0.3	1.8	0.2	0.4	0.1	1	3
(e)	1	1.8238	0.4	0	0	0.05	0.3, 1, 5	2
(e $^\infty$)	1.3105	1.82	0.3289	0	0	0.05	0.3, 1, 5	2
(f)	1	1.8	0.3	0	0	0.01, 0.1, 0.2	0.5, 1, 2	2

Table 2: Initial data and stationary configurations.

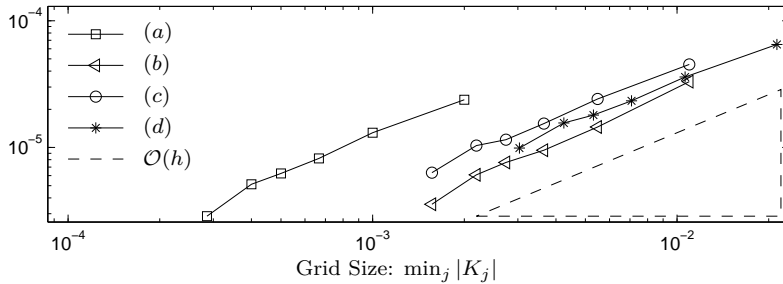


Figure 5: Experimental order of convergence.

5 Numerical Examples

In this section we test the proposed relaxation two-phase Riemann solver of section 3 as microsolver within the HMM framework of Algorithm 4.2. Two major issues are addressed: impacts of surface tension and kinetic relations on the dynamics of two-phase flows and the validation of the overall HMM.

We applied kinetic relation (11) with (13). For the mass flux estimation

$$\tilde{j}(\mathbf{V}_{\text{liq}}, \mathbf{V}_{\text{vap}}) := 0.8 \frac{v_{\text{vap}} - v_{\text{liq}}}{\tau_{\text{vap}} - \tau_{\text{liq}}} + 0.2 \frac{f(\tau_{\text{liq}}, \tau_{\text{vap}})}{-c} \quad (37)$$

was used, where $f(\tau_{\text{liq}}, \tau_{\text{vap}}) = \llbracket \psi(\tau) \rrbracket + \frac{p(\tau_{\text{liq}}) + p(\tau_{\text{vap}})}{2} \llbracket \tau \rrbracket + \frac{\tau_{\text{liq}} + \tau_{\text{vap}}}{2} (d-1) \zeta \kappa$. Note that $f(\tau_{\text{liq}}, \tau_{\text{vap}}) + k(j) = 0$ is equivalent to (11) when (7) holds. The convex combination (37) ensures (29) and was chosen in view of Remark 3.4. For the flux computation in the bulk phases we apply a local Lax–Friedrichs method [16].

5.1 Experimental Order of Convergence

The first test is devoted to the validation of the HMM. We demonstrate grid convergence of optimal order. For $\Omega = \{ \mathbf{x} \in \mathbb{R}^d \mid 0.95 < |\mathbf{x}| < 1.05 \}$, Riemann initial data (a)-(d) of Table 2 are used. Since exact solutions are not available a reference solution $\tilde{\mathbf{W}}$ was computed with $I = 500$ cells. We calculate the error

$$\epsilon_h = \int_0^T \int_{R_{\min}}^{R_{\max}} A_d(r) |\mathbf{W}_h(r, t) - \tilde{\mathbf{W}}(r, t)| \, dr \, dt$$

for the numerical solution \mathbf{W}_h on 50, 100, 150, 200, 250 and 350 cells, respectively. The end time $T = 0.01$ was reached after around 700 time steps for the finest grid.

Figure 5 shows the first order of convergence for several initial conditions and spatial dimensions. This is the optimal order that can be expected in view of the first-order scheme (34).

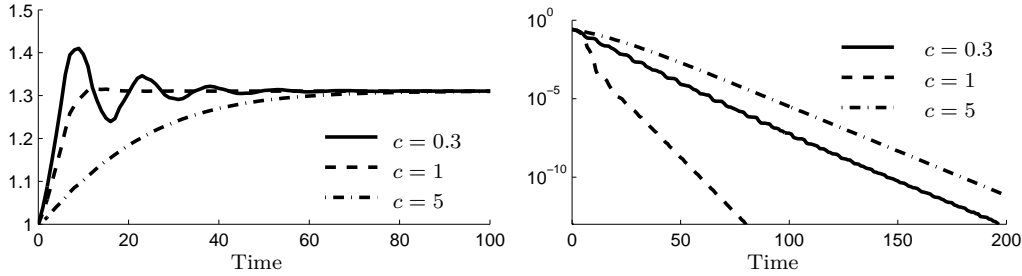


Figure 6: Evolution of the droplet radius (left) and the energy decay (right) in time.

5.2 Global Energy Release and Steady State Solutions

A transient solution should reach its steady state at $T = \infty$ and at the same time should be the minimizer of the associated energy/entropy. The total energy at time t in d -dimensional setting is given by (cf. [11])

$$\mathcal{E}(\varrho(\cdot, t), \mathbf{m}(\cdot, t)) = \int_{\Omega_{\text{liq}}(t) \cup \Omega_{\text{vap}}(t)} \varrho(\mathbf{x}, t) \psi\left(\frac{1}{\varrho(\mathbf{x}, t)}\right) + \frac{|\mathbf{m}(\mathbf{x}, t)|^2}{2\varrho(\mathbf{x}, t)} \, d\mathbf{x} + \zeta |\Gamma(t)|.$$

We have seen in Remark 2.1 that stationary two-phase solutions are determined by (15) such that the energy reaches its minimum with $\mathcal{E}_{\text{stat}} := \min \{ \mathcal{E}(\varrho, \mathbf{0}) \mid \int_{\Omega} \varrho \, d\mathbf{x} = \int_{\Omega} \varrho_0 \, d\mathbf{x} \}$.

With $\Omega = \{ \mathbf{x} \in \mathbb{R}^d \mid 0 < |\mathbf{x}| < 4 \}$ and initial conditions (e) the states in (e^∞) , Table 2, provide a stationary solution.

Figure 6 left shows that the evolution of the approximate solution with 100 cells towards a configuration with the stationary droplet diameter. This observations holds for different mobility parameters in (13). Moreover, increasing entropy dissipation via the mobility parameter seems to have a damping effect. Figure 6 right shows the global energy decay $t \mapsto \mathcal{E}(\varrho(\cdot, t), \mathbf{m})(\cdot, t) - \mathcal{E}_{\text{stat}}$. One observes the method is capable to converge to the stationary solution. The highest energy release was obtained for $c = 1$, for $c = 0.3$ the solution oscillates around the stationary solution and for $c = 5$ the final state is approached very slowly.

5.3 Evaporating Droplet

Finally we consider the dynamics for an evaporating droplet with slightly different boundary conditions. At the inner boundary (3) is still used. At the outer boundary R_{max} we apply the outflow condition $\mathbf{F}_{I+1,-}^n = \mathbf{F}(\mathbf{W}_I^n)$ to mimic an unbounded container.

Figure 7 displays the solution for $c = 1$, $\zeta = 0.1$ and initial states (f) in Table 2 with 5000 cells. As expected the droplet vanishes for this setting. Note that plateau values do not form due to the intrinsic geometry change in r . The evolution of the droplet radius for different values of mobility c and surface tension ζ are shown in Figure 8. For lower dissipation rates, the droplet evaporates faster. The same holds for higher surface tension.

References

- [1] R. Abeyaratne and J. Knowles. *Evolution of Phase Transitions: A Continuum Theory*. Cambridge University Press, 2006.
- [2] H. B. Callen. *Thermodynamics and an Introduction to Thermostatistics*. Wiley, New York, 2. edition, 1985.
- [3] C. Chalons, F. Coquel, P. Engel, and C. Rohde. Fast relaxation solvers for hyperbolic-elliptic phase transition problems. *SIAM Journal on Scientific Computing*, 34(3):A1753–A1776, 2012.

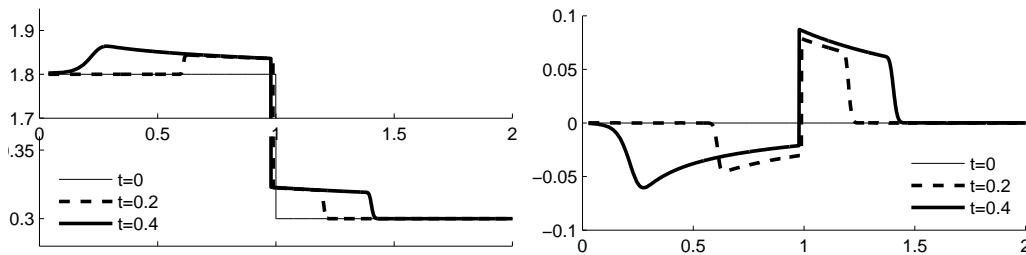


Figure 7: Solution of the evaporating droplet example. Left: density profile, right: velocity profile.

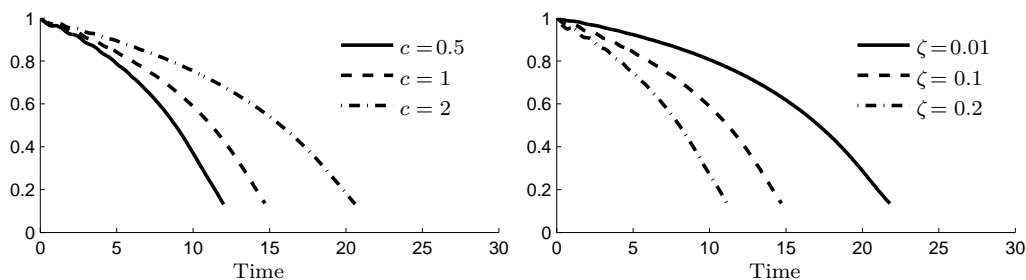


Figure 8: Evolution of the droplet radius $\Gamma(t)$. Left: $\zeta = 0.1$ and altering rates of entropy release. Right: $c = 1$ and altering surface tension coefficients.

- [4] C. Chalons, F. Coquel, and C. Marmignon. Well-balanced time implicit formulation of relaxation schemes for the Euler equations. *SIAM Journal on Scientific Computing*, 30(1):394–415, 2008.
- [5] C. Chalons, P. Engel, and C. Rohde. A conservative and convergent scheme for undercompressive shock waves. Technical report, 2012.
- [6] C. Chalons and P. Goatin. Godunov scheme and sampling technique for computing phase transitions in traffic flow modeling. *Interfaces Free Bound.*, 10(2):197–221, 2008.
- [7] C. Chalons and P. G. LeFloch. Computing undercompressive waves with the random choice scheme. Nonclassical shock waves. *Interfaces Free Bound.*, 5(2):129–158, 2003.
- [8] C. Chalons, C. Rohde, and M. Wiebe. A conservative scheme for phase boundaries in 1d. Technical report, in preparation.
- [9] A. Dressel and C. Rohde. A finite-volume approach to liquid-vapour fluids with phase transition. In *Finite volumes for complex applications V*, pages 53–68. ISTE, London, 2008.
- [10] W. Dreyer, M. Hantke, and G. Warnecke. Exact solutions to the Riemann problem for compressible isothermal Euler equations for two phase flows with and without phase transition. *Quart. Appl. Math.*, 71:509–540, 2013.
- [11] M. E. Gurtin. On a theory of phase transitions with interfacial energy. *Arch. Rational Mech. Anal.*, 87(3):187–212, 1985.
- [12] F. Jaegle, C. Rohde, and C. Zeiler. A multiscale method for compressible liquid-vapor flow with surface tension. *ESAIM: Proc.*, 38:387–408, 2012.
- [13] F. Kissling and C. Rohde. The computation of nonclassical shock waves with a heterogeneous multiscale method. *Netw. Heterog. Media*, 5(3):661–674, 2010.
- [14] P. G. LeFloch. *Hyperbolic Systems of Conservation Laws*. Lectures in Mathematics ETH Zürich. Birkhäuser Verlag, Basel, 2002. The theory of classical and nonclassical shock waves.

- [15] P. G. LeFloch and M. D. Thanh. Non-classical Riemann solvers and kinetic relations. II. An hyperbolic-elliptic model of phase-transition dynamics. *Proc. Roy. Soc. Edinburgh Sect. A*, 132(1):181–219, 2002.
- [16] R. J. LeVeque. *Finite Volume Methods for Hyperbolic Problems*. Cambridge Univ. Press, Cambridge, repr. edition, 2007.
- [17] S. Li. Weno schemes for cylindrical and spherical grid. In H. R. Arabnia, editor, *CSC*, pages 177–183. CSREA Press, 2006.
- [18] C. Merkle and C. Rohde. The sharp-interface approach for fluids with phase change: Riemann problems and ghost fluid techniques. *M2AN Math. Model. Numer. Anal.*, 41(6):1089–1123, 2007.
- [19] L. Truskinovsky. Kinks versus shocks. In *Shock induced transitions and phase structures in general media*, pages 185–229. Springer, New York, 1993.
- [20] E. Weinan, B. Engquist, X. Li, W. Ren, and E. Vanden-Eijnden. Heterogeneous multiscale methods: a review. *Commun. Comput. Phys.*, 2(3):367–450, 2007.
- [21] X. Zhong, T. Y. Hou, and P. G. LeFloch. Computational methods for propagating phase boundaries. *J. Comput. Phys.*, 124(1):192–216, 1996.

Christian Rohde
Pfaffenwaldring 57
70569 Stuttgart
Germany

E-Mail: Christian.Rohde@mathematik.uni-stuttgart.de

WWW: www.mathematik.uni-stuttgart.de/fak8/ians/lehrstuhl/LstAngMath

Christoph Zeiler
Pfaffenwaldring 57
70569 Stuttgart
Germany

E-Mail: Christoph.Zeiler@mathematik.uni-stuttgart.de

WWW: www.mathematik.uni-stuttgart.de/fak8/ians/lehrstuhl/LstAngMath

Erschienenene Preprints ab Nummer 2007/2007-001

Komplette Liste: <http://www.mathematik.uni-stuttgart.de/preprints>

- 2013-014 *Rohde, C.; Zeiler, C.:* A Relaxation Riemann Solver for Compressible Two-Phase Flow with Phase Transition and Surface Tension
- 2013-013 *Moroianu, A.; Semmelmann, U.:* Generalized Killing spinors on Einstein manifolds
- 2013-012 *Moroianu, A.; Semmelmann, U.:* Generalized Killing Spinors on Spheres
- 2013-011 *Kohls, K.; Rösch, A.; Siebert, K.G.:* Convergence of Adaptive Finite Elements for Control Constrained Optimal Control Problems
- 2013-010 *Corli, A.; Rohde, C.; Schleper, V.:* Parabolic Approximations of Diffusive-Dispersive Equations
- 2013-009 *Nava-Yazdani, E.; Polthier, K.:* De Casteljau's Algorithm on Manifolds
- 2013-008 *Bächle, A.; Margolis, L.:* Rational conjugacy of torsion units in integral group rings of non-solvable groups
- 2013-007 *Knarr, N.; Stroppel, M.J.:* Heisenberg groups over composition algebras
- 2013-006 *Knarr, N.; Stroppel, M.J.:* Heisenberg groups, semifields, and translation planes
- 2013-005 *Eck, C.; Kutter, M.; Sändig, A.-M.; Rohde, C.:* A Two Scale Model for Liquid Phase Epitaxy with Elasticity: An Iterative Procedure
- 2013-004 *Griesemer, M.; Wellig, D.:* The Strong-Coupling Polaron in Electromagnetic Fields
- 2013-003 *Kabil, B.; Rohde, C.:* The Influence of Surface Tension and Configurational Forces on the Stability of Liquid-Vapor Interfaces
- 2013-002 *Devroye, L.; Ferrario, P.G.; Györfi, L.; Walk, H.:* Strong universal consistent estimate of the minimum mean squared error
- 2013-001 *Kohls, K.; Rösch, A.; Siebert, K.G.:* A Posteriori Error Analysis of Optimal Control Problems with Control Constraints
- 2012-018 *Kimmerle, W.; Konovalov, A.:* On the Prime Graph of the Unit Group of Integral Group Rings of Finite Groups II
- 2012-017 *Stroppel, B.; Stroppel, M.:* Desargues, Doily, Dualities, and Exceptional Isomorphisms
- 2012-016 *Moroianu, A.; Pilca, M.; Semmelmann, U.:* Homogeneous almost quaternion-Hermitian manifolds
- 2012-015 *Steinke, G.F.; Stroppel, M.J.:* Simple groups acting two-transitively on the set of generators of a finite elation Laguerre plane
- 2012-014 *Steinke, G.F.; Stroppel, M.J.:* Finite elation Laguerre planes admitting a two-transitive group on their set of generators
- 2012-013 *Diaz Ramos, J.C.; Dominguez Vázquez, M.; Kollross, A.:* Polar actions on complex hyperbolic spaces
- 2012-012 *Moroianu, A.; Semmelmann, U.:* Weakly complex homogeneous spaces
- 2012-011 *Moroianu, A.; Semmelmann, U.:* Invariant four-forms and symmetric pairs
- 2012-010 *Hamilton, M.J.D.:* The closure of the symplectic cone of elliptic surfaces
- 2012-009 *Hamilton, M.J.D.:* Iterated fibre sums of algebraic Lefschetz fibrations
- 2012-008 *Hamilton, M.J.D.:* The minimal genus problem for elliptic surfaces
- 2012-007 *Ferrario, P.:* Partitioning estimation of local variance based on nearest neighbors under censoring
- 2012-006 *Stroppel, M.:* Buttons, Holes and Loops of String: Lacing the Doily

- 2012-005 *Hantsch, F.*: Existence of Minimizers in Restricted Hartree-Fock Theory
- 2012-004 *Grundhöfer, T.; Stoppel, M.; Van Maldeghem, H.*: Unitals admitting all translations
- 2012-003 *Hamilton, M.J.D.*: Representing homology classes by symplectic surfaces
- 2012-002 *Hamilton, M.J.D.*: On certain exotic 4-manifolds of Akhmedov and Park
- 2012-001 *Jentsch, T.*: Parallel submanifolds of the real 2-Grassmannian
- 2011-028 *Spreer, J.*: Combinatorial 3-manifolds with cyclic automorphism group
- 2011-027 *Griesemer, M.; Hantsch, F.; Wellig, D.*: On the Magnetic Pekar Functional and the Existence of Bipolarons
- 2011-026 *Müller, S.*: Bootstrapping for Bandwidth Selection in Functional Data Regression
- 2011-025 *Felber, T.; Jones, D.; Kohler, M.; Walk, H.*: Weakly universally consistent static forecasting of stationary and ergodic time series via local averaging and least squares estimates
- 2011-024 *Jones, D.; Kohler, M.; Walk, H.*: Weakly universally consistent forecasting of stationary and ergodic time series
- 2011-023 *Györfi, L.; Walk, H.*: Strongly consistent nonparametric tests of conditional independence
- 2011-022 *Ferrario, P.G.; Walk, H.*: Nonparametric partitioning estimation of residual and local variance based on first and second nearest neighbors
- 2011-021 *Eberts, M.; Steinwart, I.*: Optimal regression rates for SVMs using Gaussian kernels
- 2011-020 *Frank, R.L.; Geisinger, L.*: Refined Semiclassical Asymptotics for Fractional Powers of the Laplace Operator
- 2011-019 *Frank, R.L.; Geisinger, L.*: Two-term spectral asymptotics for the Dirichlet Laplacian on a bounded domain
- 2011-018 *Hänel, A.; Schulz, C.; Wirth, J.*: Embedded eigenvalues for the elastic strip with cracks
- 2011-017 *Wirth, J.*: Thermo-elasticity for anisotropic media in higher dimensions
- 2011-016 *Höllig, K.; Hörner, J.*: Programming Multigrid Methods with B-Splines
- 2011-015 *Ferrario, P.*: Nonparametric Local Averaging Estimation of the Local Variance Function
- 2011-014 *Müller, S.; Dippon, J.*: k -NN Kernel Estimate for Nonparametric Functional Regression in Time Series Analysis
- 2011-013 *Knarr, N.; Stoppel, M.*: Unitals over composition algebras
- 2011-012 *Knarr, N.; Stoppel, M.*: Baer involutions and polarities in Moufang planes of characteristic two
- 2011-011 *Knarr, N.; Stoppel, M.*: Polarities and planar collineations of Moufang planes
- 2011-010 *Jentsch, T.; Moroianu, A.; Semmelmann, U.*: Extrinsic hyperspheres in manifolds with special holonomy
- 2011-009 *Wirth, J.*: Asymptotic Behaviour of Solutions to Hyperbolic Partial Differential Equations
- 2011-008 *Stoppel, M.*: Orthogonal polar spaces and unitals
- 2011-007 *Nagl, M.*: Charakterisierung der Symmetrischen Gruppen durch ihre komplexe Gruppenalgebra
- 2011-006 *Solanes, G.; Teufel, E.*: Horo-tightness and total (absolute) curvatures in hyperbolic spaces
- 2011-005 *Ginoux, N.; Semmelmann, U.*: Imaginary Kählerian Killing spinors I

- 2011-004 *Scherer, C.W.; Köse, I.E.*: Control Synthesis using Dynamic D -Scales: Part II — Gain-Scheduled Control
- 2011-003 *Scherer, C.W.; Köse, I.E.*: Control Synthesis using Dynamic D -Scales: Part I — Robust Control
- 2011-002 *Alexandrov, B.; Semmelmann, U.*: Deformations of nearly parallel G_2 -structures
- 2011-001 *Geisinger, L.; Weidl, T.*: Sharp spectral estimates in domains of infinite volume
- 2010-018 *Kimmerle, W.; Konovalov, A.*: On integral-like units of modular group rings
- 2010-017 *Gauduchon, P.; Moroianu, A.; Semmelmann, U.*: Almost complex structures on quaternion-Kähler manifolds and inner symmetric spaces
- 2010-016 *Moroianu, A.; Semmelmann, U.*: Clifford structures on Riemannian manifolds
- 2010-015 *Grafarend, E.W.; Kühnel, W.*: A minimal atlas for the rotation group $SO(3)$
- 2010-014 *Weidl, T.*: Semiclassical Spectral Bounds and Beyond
- 2010-013 *Stroppel, M.*: Early explicit examples of non-desarguesian plane geometries
- 2010-012 *Effenberger, F.*: Stacked polytopes and tight triangulations of manifolds
- 2010-011 *Györfi, L.; Walk, H.*: Empirical portfolio selection strategies with proportional transaction costs
- 2010-010 *Kohler, M.; Krzyżak, A.; Walk, H.*: Estimation of the essential supremum of a regression function
- 2010-009 *Geisinger, L.; Laptev, A.; Weidl, T.*: Geometrical Versions of improved Berezin-Li-Yau Inequalities
- 2010-008 *Poppitz, S.; Stroppel, M.*: Polarities of Schellhammer Planes
- 2010-007 *Grundhöfer, T.; Krinn, B.; Stroppel, M.*: Non-existence of isomorphisms between certain unitals
- 2010-006 *Höllig, K.; Hörner, J.; Hoffacker, A.*: Finite Element Analysis with B-Splines: Weighted and Isogeometric Methods
- 2010-005 *Kaltenbacher, B.; Walk, H.*: On convergence of local averaging regression function estimates for the regularization of inverse problems
- 2010-004 *Kühnel, W.; Solanes, G.*: Tight surfaces with boundary
- 2010-003 *Kohler, M.; Walk, H.*: On optimal exercising of American options in discrete time for stationary and ergodic data
- 2010-002 *Gulde, M.; Stroppel, M.*: Stabilizers of Subspaces under Similitudes of the Klein Quadric, and Automorphisms of Heisenberg Algebras
- 2010-001 *Leitner, F.*: Examples of almost Einstein structures on products and in cohomogeneity one
- 2009-008 *Griesemer, M.; Zenk, H.*: On the atomic photoeffect in non-relativistic QED
- 2009-007 *Griesemer, M.; Moeller, J.S.*: Bounds on the minimal energy of translation invariant n -polaron systems
- 2009-006 *Demirel, S.; Harrell II, E.M.*: On semiclassical and universal inequalities for eigenvalues of quantum graphs
- 2009-005 *Bächle, A.; Kimmerle, W.*: Torsion subgroups in integral group rings of finite groups
- 2009-004 *Geisinger, L.; Weidl, T.*: Universal bounds for traces of the Dirichlet Laplace operator
- 2009-003 *Walk, H.*: Strong laws of large numbers and nonparametric estimation
- 2009-002 *Leitner, F.*: The collapsing sphere product of Poincaré-Einstein spaces
- 2009-001 *Brehm, U.; Kühnel, W.*: Lattice triangulations of E^3 and of the 3-torus

- 2008-006 *Kohler, M.; Krzyżak, A.; Walk, H.:* Upper bounds for Bermudan options on Markovian data using nonparametric regression and a reduced number of nested Monte Carlo steps
- 2008-005 *Kaltenbacher, B.; Schöpfer, F.; Schuster, T.:* Iterative methods for nonlinear ill-posed problems in Banach spaces: convergence and applications to parameter identification problems
- 2008-004 *Leitner, F.:* Conformally closed Poincaré-Einstein metrics with intersecting scale singularities
- 2008-003 *Effenberger, F.; Kühnel, W.:* Hamiltonian submanifolds of regular polytope
- 2008-002 *Hertweck, M.; Höfert, C.R.; Kimmerle, W.:* Finite groups of units and their composition factors in the integral group rings of the groups $PSL(2, q)$
- 2008-001 *Kovarik, H.; Vugalter, S.; Weidl, T.:* Two dimensional Berezin-Li-Yau inequalities with a correction term
- 2007-006 *Weidl, T.:* Improved Berezin-Li-Yau inequalities with a remainder term
- 2007-005 *Frank, R.L.; Loss, M.; Weidl, T.:* Polya's conjecture in the presence of a constant magnetic field
- 2007-004 *Ekholm, T.; Frank, R.L.; Kovarik, H.:* Eigenvalue estimates for Schrödinger operators on metric trees
- 2007-003 *Lesky, P.H.; Racke, R.:* Elastic and electro-magnetic waves in infinite waveguides
- 2007-002 *Teufel, E.:* Spherical transforms and Radon transforms in Moebius geometry
- 2007-001 *Meister, A.:* Deconvolution from Fourier-oscillating error densities under decay and smoothness restrictions